Solvent-mediated modification of thermodynamics and kinetics of monoethanolamine regeneration reaction in amine-stripping carbon capture: computational chemistry study

OPEN ACCESS

Solvent-mediated modification of thermodynamics and kinetics of monoethanolamine regeneration reaction in amine-stripping carbon capture: computational chemistry study

N.D. Afify[1,a] and M.B. Sweatman[1]

[1] *Institute for Materials and Processes, School of Engineering, The University of Edinburgh, Edinburgh EH9 3FB, UK*

[1]Corresponding author: N.Afify@ed.ac.uk

A major limitation of amine-based post-combustion carbon capture technology is the necessity to regenerate amines at high temperatures, which dramatically increases the operating costs. This paper concludes the effect of solvent choice as a possible route to modify the thermodynamics and kinetics characterizing the involved amine regeneration reactions, and discusses whether these modifications can be economically beneficial. We report experimentally-benchmarked computational chemistry calculations of monoethanolamine (MEA) regeneration reactions employing aqueous and non-aqueous solvents with a wide range of dielectric constants. Unlike previous studies, our improved computational chemistry framework could accurately reproduce the right experimental activation energy of zwitterion formation. From the predicted reactions thermodynamics and kinetics, the use of non-aqueous solvents with small dielectric constants led to reductions in regeneration Gibbs free energies, activation barriers and enthalpy changes. This can reduce energy consumption, and gives an opportunity to run desorption columns at relatively lower temperatures, thus offering the possibility of relying on low-grade waste heat as an energy input.

I. INTRODUCTION

Amine-based post-combustion carbon capture (PCCC) technology is currently one of the most mature routes in the world fight against Climate Change.[1] This technology involves a continuous cyclic process of CO_2 molecules absorption and desorption by an amine.[2-3] An exhaust gas containing CO_2 passes through the bottom of an absorption column, where it comes into contact with an amine solution. The CO_2 molecules then react with amine molecules, forming carbamate at temperatures ranging from 40°C to 60°C at atmospheric pressure.[2-3] The CO_2-rich amine solution then flows to a stripping column, where it undergoes an endothermic regeneration reaction to reproduce the spent amine and a purified CO_2 stream for storage. The remaining amine-rich solution then exits the bottom of the stripping column and recirculates back to the absorption column for the next cycle.

The above amine-based PCCC technology suffers from high operating energy costs, since it requires regenerating the spent amine at high temperatures, typically between 120°C and 140°C at 1-2 bar.[2,4-7] Reduction of these energy

27 costs has become an important research area.[2-8] In the past few years, researchers followed several approaches to

28 reduce such large energy costs. One approach was to replace conventional steam heating by microwave heating[2,9-

29 11] or frequency-tuned infrared preferential heating[12] of amine solutions. Another research approach used different

30 amine types[13-18], including monoethanolamine (MEA), diethanolamine (DEA), triethanolamine (TEA),

31 diisopropanolamine (DIPA), 2-amino-2-methyl-1-propanol (AMP), and methyldiethanolamine (MDEA). A third

32 research direction to reduce amine regeneration energy consumption focused on evaluation of several aqueous[19-22]

33 and non-aqueous solvents.[23-30]

34 In the present computational work, we are interested in understanding if the use of non-aqueous solvents with small

35 dielectric constants can lead to amine regeneration processes with less energy consumption or lower regeneration

36 temperatures requirements, when compared to the use of water as a solvent. Our study selected monoethanolamine

37 (MEA) as it is the most industrially used amine.[11] To obtain a clear picture on the role of solvent we studied several

38 solvents with a wide range of static dielectric constants, ranging from 7.43 up to 108.94 at room temperature. Our

39 solvents included tetrahydrofuran (THF), t-butanol, 1-pentanol, acetone, ethanol, methanol, dimethyl sulfoxide

40 (DMSO), water, and formamide.

41 **II. COMPUTATIONAL DETAILS**

42 Although our initial testing simulations were carried out using the GAUSSIAN 16[33] and General Atomic and

43 Molecular Electronic Structure System GAMESS[34] codes, for performance reasons, our production calculations

44 were fully carried out using the ORCA 5.0.3 code.[35] Our computational work was carried out on the Cirrus and

45 Eddie high performance computing clusters available at the University of Edinburgh. Before looking into the effect

46 of solvent choice on the thermodynamics and kinetics of involved amine regeneration reactions, it was very

47 important to benchmark the accuracy of our computational chemistry calculations against experimental data. This

48 was carried out through a comprehensive testing of the mechanisms and kinetics characterizing the CO_2 reaction

49 with MEA in presence of water as a solvent.

50 While geometry optimization, intrinsic reaction coordinate (IRC)[35], and frequency calculations were carried out

51 using density function theory (DFT), final single-point electronic energies were computed using the domain-based

52 local pair natural orbital coupled-cluster method DLPNO-CCSD(T)[35,51] implemented in the ORCA code. In all

53 calculations, implicit solvent effects were included using the polarizable continuum model (PCM)[31] in conjunction

54 with the Pauling atomic radii.[32] The Def2-TZVP basis set[35] was employed in both DFT and DLPNO-CCSD(T)

55 calculations. To reach the most accurate computational framework we evaluated several DFT functionals. Although

56 most of previous computational studies[36-46] were carried out using the most commonly used B3LYP hybrid

57 functional, the B3LYP functional has recently turned out to be of average performance when it comes to

58 thermochemistry calculations.[53] In addition to B3LYP, we tested several meta-GGA and hybrid meta-GGA

59 functionals, including TPSS, TPSSh, TPSS0, M06, M062X, M06L, rM06L, and SCANfunc, and range-separated

60 hybrid functionals, including wB97, wB97X, wB97X-D3, wB97X-D4, wB97X-D3BJ, and CAM-B3LYP.[35] Gibbs

61 free energies, activation barriers and enthalpy changes were calculated by combining the DLPNO-CCSD(T)

62 electronic energies and DFT vibrational analysis results.

63 Our DFT calculations included the zero-point energy and geometrical counterpoise corrections.[54] We have also

64 evaluated the effect of including the Grimme's dispersion correction (D3BJ version)[55]. As it will be discussed later,

65 for the current chemical reactions including the dispersion correction caused more deviation from experimental

66 activation energies. Therefore, we have decided to proceed only with the geometrical counterpoise correction, since

67 it produces the best agreement with experimental activation energies.

68 **III. RESULTS AND DISCUSSION**

69 **A. Accuracy of thermochemistry predictions**

70 In this section we evaluate the accuracy of our computational framework in reproducing the correct reaction

71 mechanisms and experimental activation energy in the case of water as a solvent. In agreement with all previous

72 computational studies[36-46], all evaluated DFT functionals have predicted the same reaction mechanisms. In Fig. 1

73 we report the DFT optimized molecular geometries in the major reaction steps in the case of the TPSS0 functional.

74 Relative electronic energies corresponding to these geometries are shown in the potential energy surface reported

75 in Fig. 2.

We first discuss the possible reactions mechanisms. From steps 1, 2 and 3 in Fig. 1, we can see that one CO_2 molecule reacts with one MEA molecule to form zwitterion. This zwitterion can then enter one of the following two routes. The first possibility is the formation of carbamic acid (steps 3, 4 and 5). The second possibility is the reaction of zwitterion with a nearby MEA molecule to form carbamate ion pairs (steps 6, 7 and 8). From the potential energy surface reported in Fig. 2 we can confirm that the formation of carbamic acid is energetically unfavourable, in agreement with previous studies. In summary, the main reactions steps involved in amine-based carbon capture are the formation of zwitterion and the subsequent formation of carbamate ion pairs. This mechanism agrees well with several computational studies.[36-46]
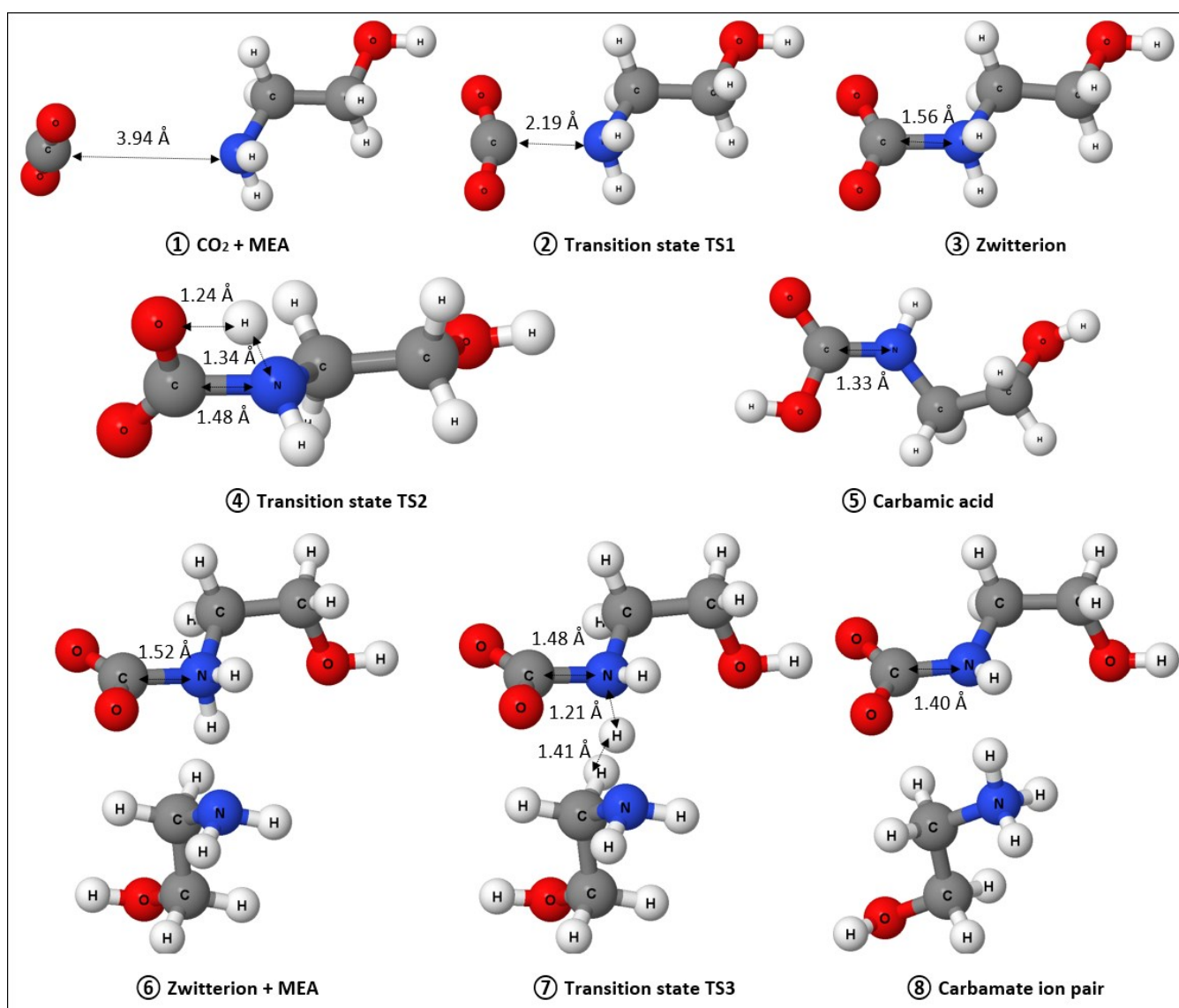
Fig. 1. DFT optimized molecular geometries of reactants, products, and transition states involved in reaction of CO_2 with MEA in presence of water as solvent. Reported geometries correspond to the TPSS0/ Def2-TZVP level of theory.

4

87
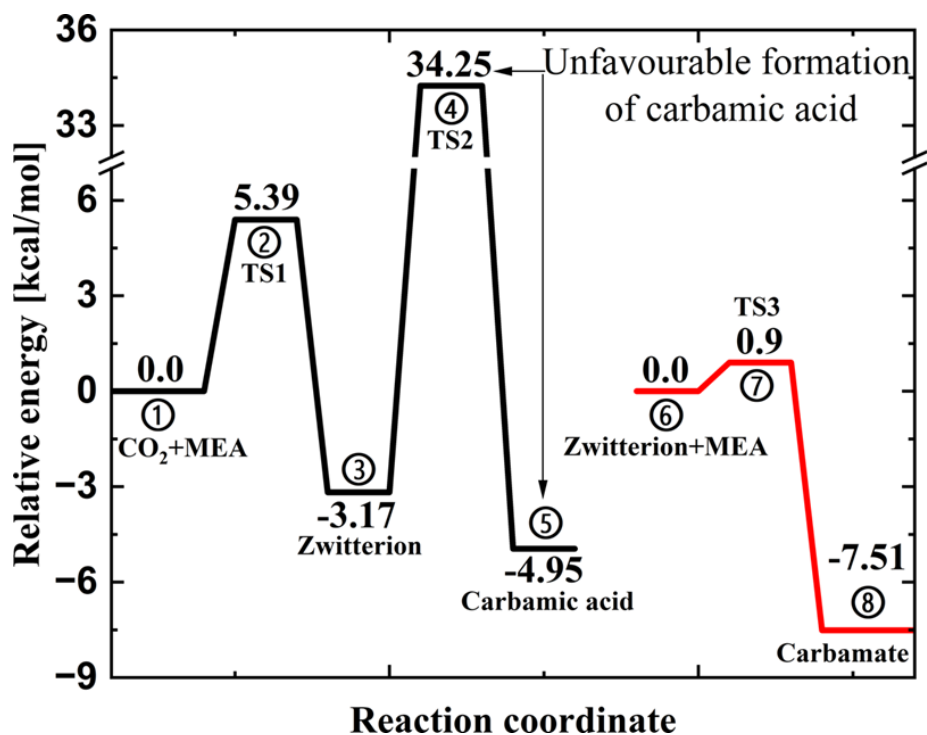
Fig. 2. Relative potential energy surface corresponding to the molecular geometries reported in Fig. 1. Reported values correspond to single-point electronic energies computed at the DLPNO-CCSD(T)/Def2-TZVP level of theory.

In Table 1 we report the activation energies for zwitterion and carbamate formation (i.e. forward reactions) and regeneration (i.e. backword reactions). These activation energies were obtained by combining the DLPNO-CCSD(T) electronic energies and DFT frequency calculations at 298.15 K and 1 bar. In Table S1 (Supplementary Material) we compare these values to activation energies calculated purely from DFT electronic energies and frequency calculations. Table S1 also contains the activation energies for the unfavourable carbamic acid reaction route. At this point, it is important to decide which DFT functional produces the most accurate results. Experimental activation energies for zwitterion formation were reported by Ali et al.[47] (11.14 kcal/mol) and Alper et al.[48] (11.16 kcal/mol) using the direct stopped-flow technique. From Table 1, it is clear that the TPSS0 was the best DFT functional able to accurately predict the experimental activation energy of zwitterion formation.

In the following, we give an additional reason why the above result is indeed important. Some previous computational chemistry studies compared their predicted activation energies for zwitterion formation to the above experimental studies.[36-39] Unfortunately, authors in these studies compared their predicted activation energies to the

5

105 wrong experimental value, namely 12.4 kcal/mol. The used experimental activation energy in fact corresponds to

106 the case of the AMP amine, not MEA.[47,49] This point was very important to comment on in order to avoid potential

107 confusion in future studies.

108 **Table 1.** Activation energies (kcal/mol) obtained by combining the DFT frequency calculations at 298.15 K and DLPNO-
109 CCSD(T) electronic energies. All calculation used water as a solvent and employed the Def2-TZVP basis set.

	Zwitterion		Carbamate	
	Forward	Backward	Forward	Backward
B3LYP	9.97	5.09	0.13	6.71
TPSS	8.19	4.20	0.10	6.39
TPSSh	10.80	4.56	-0.04	6.67
TPSS0	**11.13**	**4.74**	**-0.22**	**6.96**
M06	8.10	5.61	0.81	5.35
M062X	7.14	4.86	0.08	4.87
M06L	7.79	5.37	-0.97	5.86
rM06L	8.86	5.36	-0.72	6.96
SCANfunc	6.36	3.65	-1.27	5.30
wB97	8.17	5.00	0.79	5.47
wB97X	8.57	4.93	0.07	5.77
wB97X-D3	9.71	4.93	0.06	5.50
wB97X-D4	8.83	4.87	-0.08	5.57
wB97X-D3BJ	8.86	4.81	-0.20	5.61
CAM-B3LYP	9.48	4.84	-0.19	5.70

110 As mentioned above in the Computational Details section, our DFT calculations evaluated the effects of including

111 the geometrical counterpoise[54] and Grimme's dispersion[55] corrections. In the following, we justify our decision to

112 consider results obtained by incorporating only the geometrical counterpoise correction. In Table S3

113 (Supplementary Material) we report the effect of including these two corrections on the zwitterion formation

114 activation energy. Results are reported for the case of water as solvent, and B3LYP, TPSS, TPSSh and TPSS0 DFT

115 functionals. In this table, ΔE_{exp} represents the deviation of the calculated activation energy from experimental value

116 (11.15 kcal/mol). Inspection of the results reported in Table S3 reveals the following four cases.

117 Let us first discard both the counterpoise and dispersion corrections. In this case, the TPSS0 functional produces

118 the best agreement with the experimental activation energy (ΔE_{exp} = 0.46 kcal/mol), followed by TPSSh (ΔE_{exp} = 0.76

119 kcal/mol) and B3LYP (ΔE_{exp} = 1.61 kcal/mol). In the second case, we included both the counterpoise and dispersion

120 corrections. This makes B3LYP the most accurate functional (ΔE_{exp} = 1.68 kcal/mol), followed by TPSSh (ΔE_{exp} =

121 2.24 kcal/mol) and TPSS (ΔE_{exp} = 2.76 kcal/mol). In the third case, we included only the dispersion correction. In

122 this case, again the B3LYP functional comes best (ΔE_{exp} = 1.68 kcal/mol), followed by TPSS (ΔE_{exp} = 2.03 kcal/mol)

123 and TPSS0 (ΔE_{exp} = 2.54 kcal/mol). In the fourth case, we included only the counterpoise correction. This puts the

124   TPSS0 functional as the absolute best (ΔE_{exp} = 0.02 kcal/mol) functional, followed by the TPSSh (ΔE_{exp} = 0.35

125   kcal/mol) and B3LYP (ΔE_{exp} = 1.18 kcal/mol) functionals.

126   The above analysis reveals the sensitivity of the obtained activation energies to the employed DFT functional and

127   inclusion of dispersion and counterpoise corrections. In this study, we were looking for the best computational

128   framework able to produce best agreement with experimental data. Given results of the above analysis, we believe

129   the use of the TPSS0 functional in conjunction with the counterpoise corrections is effectively the best choice for

130   studying the current chemical reactions. This is consistent with a recent computational chemistry study[56], which

131   showed that the hybrid B3LYP functional, having 20% HF exchange, presented a poor performance compared to

132   hybrid meta-GGA functionals having 25% HF exchange.

133   **B. Effect of solvent choice on regeneration thermodynamics and kinetics**

134   In this section we comment on the effect of solvent choice on thermodynamics and kinetics of amine regeneration

135   reactions. As discussed above, the regeneration reaction consists of two main steps. The first step involves two

136   amine molecules, where carbamate anion abstracts one proton from another protonated amine molecule, resulting

137   in zwitterion and neutral amine molecules. The second step is the liberation of CO_2 molecule from zwitterion,

138   resulting in unreacted CO_2 and amine molecules. In Table 2 we report the Gibbs free energies and activation energy

139   barriers corresponding to these two steps, in addition to the total regeneration enthalpy change. In Table 2 we also

140   report experimental specific heat capacities of the different solvents, taken from the Springer Materials database.

141   First, we discuss the dependence of reactions thermodynamics on the solvent type. From the computed Gibbs free

142   energies, we can see that the regeneration of zwitterion from carbamate (first step) is an endothermic reaction. On

143   contrary, the regeneration of amine from zwitterion (second step) is spontaneous reaction, as evidenced from the

144   negative Gibbs free energy. From the enthalpy changes reported in Table 2, it is very clear that using non-aqueous

145   solutions with small dielectric constants can reduce the amount of input energy required to achieve the amine

146   regeneration reaction. It is important to point out that the reduction in the required energy input cannot be explained

147   only by the differences in specific heat capacities reported in Table 2. For example, the use of formamide would

148   require more energy input than water, although formamide has almost half of the heat capacity of water.

149 **Table 2.** Effect of solvent choice on thermodynamics and kinetics of amine regeneration reactions. These results were obtained
150 by combining the DFT frequency calculations at 298.15 K and DLPNO-CCSD(T) electronic energies. DFT calculations were
151 carried out at the TPSS0/Def2-TZVP level of theory.

Solvent	Dielectric constant	Step 1: carbamate to zwitterion		Step 2: zwitterion to MEA		Enthalpy change	Specific heat capacity
		Gibbs free energy [kcal/mol]	Activation energy [kcal/mol]	Gibbs free energy [kcal/mol]	Activation energy [kcal/mol]	[kcal/mol]	[J/gK]
THF	7.43	2.38	3.20	-7.77	1.95	0.43	1.770
t-butanol	12.47	4.18	4.46	-5.94	3.05	3.47	2.359
1-pentanol	15.13	4.67	4.81	-7.98	3.38	4.90	2.336
Acetone	20.49	5.35	5.36	-7.70	3.79	5.96	2.131
Ethanol	24.85	5.75	5.70	-7.19	4.01	6.49	2.512
Methanol	32.61	6.26	6.14	-4.76	4.25	6.48	2.508
DMSO	46.83	7.00	6.82	-6.62	4.50	7.68	1.960
Water	78.36	7.18	6.96	-6.39	4.74	8.22	4.188
Formamide	108.94	7.09	6.85	-6.20	4.82	8.45	2.388

152 This finding agrees well with recent experimental study.[8] In this study, Bougie et al. studies several solvents

153 including a mixture of ethylene glycol and 1-propanol, diethylene glycol monoethyl ether (DEGMEE), and N-

154 methylformamide (NMF). They found that energy consumption reduces from 3630 kJ/mol in the case of water

155 (dielectric constants of 78.355) to 929 kJ/mol in the case of DEGMEE (dielectric constant of 12.6). The findings in

156 this experimental study fully support our computational results.

157 Now we focus on the effect of solvent choice on the kinetics of regeneration reaction. Activation energies for the

158 two regeneration steps are reported in Table 2. In Fig. 3a we show the dependence of these activation energies on

159 the solvent dielectric constant. As we can see, regeneration of zwitterion from carbamate exhibits higher activation

160 energies compared to the regeneration of MEA from zwitterion. This indicates that the regeneration of zwitterion

161 from carbamate is the rate-determining regeneration step regardless of the employed solvent. Going from

162 formamide to THF we can see that the activation energy decreases as a function of the solvent dielectric constant.

163 To confirm the dependence of activation energy on the solvent, in Fig. 3b we report bond order analysis of the

164 N_{MEA}-C_{CO2} bonds in zwitterion and carbamate. This bond order analysis gives us an idea about the relative chemical

165 stabilities of zwitterion and carbamate. Bond order analysis was carried out using the Löwdin population analysis[50]

166 implemented in the ORCA code.[35] From Fig. 3b it can be understood that the N_{MEA}-C_{CO2} bond in zwitterion is

167 covalent in nature, and becomes relatively weaker when we use solvents with small dielectric constant. The N_{MEA}-

168 C_{CO2} bond in carbamate have values between 1.4 and 1.46, depending on the employed solvent, which suggests it

169   is partially ionic bond. Thus, the N_{MEA}-C_{CO2} bond in carbamate is much stronger than that in zwitterion, which

170   explains why zwitterion regeneration is the rate-determining step, which is indeed documented in Fig. 3a.
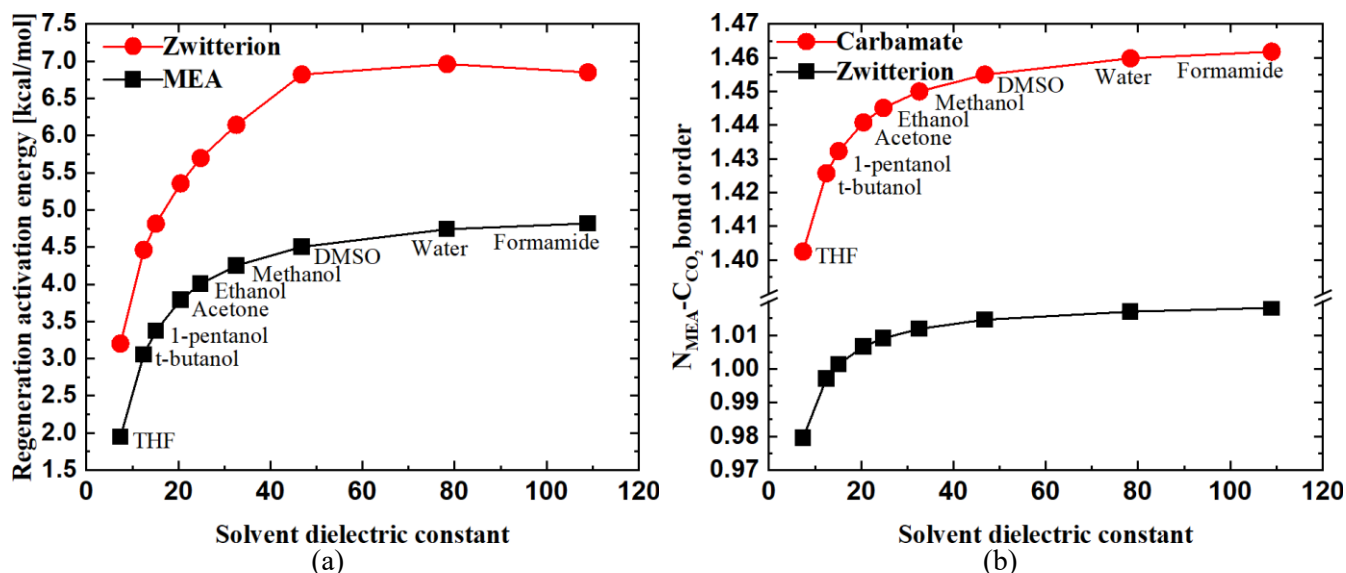

171   **Fig. 3.** (a) Effect of the solvent dielectric properties on the activation energies of the two regeneration reaction steps. Red circles
172   and black squares correspond to converting carbamate to zwitterion and zwitterion to MEA. (b) Relative chemical stabilities
173   of zwitterion and carbamate as calculated from bond order analysis of the N_{MEA}-C_{CO2} bond.
174

175   In the following we seek to understand how the reduction in regeneration activation energy reported in Table 2 and

176   Fig. 3a will play out in terms of heat input requirements. Higher activation energy implies that solution should be

177   heated at higher temperature, thus molecules will have sufficient energy to cross energy barrier. Lowering this

178   temperature will lower the rate at which carbamate decomposed into amine and CO_2. The fact that non-aqueous

179   solutions with low dielectric constants exhibit lower activation energies means that amines can be regenerated in

180   these solutions at lower temperatures compared to aqueous solutions, assuming the same amine regeneration rate.

181   In Fig. 4 we report amine regeneration rate constant as a function of temperature for the different solvents. The

182   MEA regeneration reaction rate constants were calculated using the Eyring equation.[51] From this figure, the

183   regeneration reaction rate at any regeneration temperature increases by decreasing the solvent dielectric constant.

184   This agrees well with the recent experimental results obtained by Bougie et al.[8] In this experimental study it was

185   found that the amount of desorbed CO_2 in the case of the DEGMEE solvent (dielectric constant of 12.6) was much

186   higher than the case of water (dielectric constant of 78.4). Similarly, the amount of desorbed CO_2 in the case of

187 water was much higher than the case of the NMF solvent (dielectric constant of 182.0). Thus, our computational

188 regeneration kinetics results are in line with those obtained experimentally.[8]

189 Taking into account that typical regeneration temperature in the case of water is about 140°C[2,4-7], we can now

190 estimate from Fig. 4 what regeneration temperatures are required for other solvents, keeping the same regeneration

191 rate constant. From this figure (see dashed lines) it is possible to achieve MEA regeneration reaction at much lower

192 temperatures if we use solvents with low dielectric constants. For example, in the case of acetone as a solvent the

193 regeneration temperature would be as low as 50°C, which is much less than the 140°C required in the case of water.
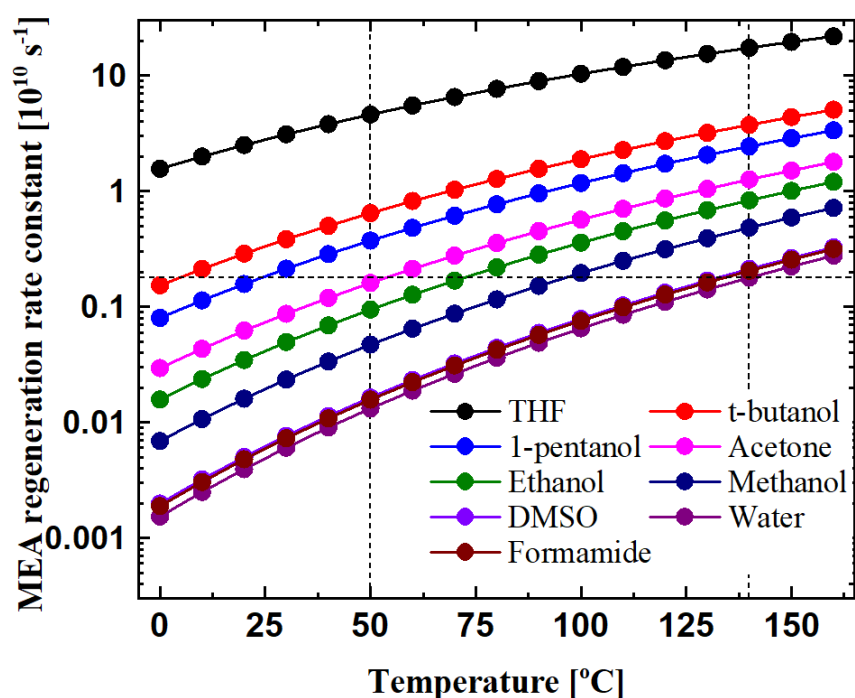
194
195
196 **Fig. 4.** MEA regeneration reaction rate constant as a function of temperature and solvent dielectric constant.
197

198 The solvent vapour pressure is a very important factor to consider when judging the suitability of a certain solvent

199 for carbon capture applications. Acetone for example has a vapour pressure of 30.6 kPa at 25 °C, which is much

200 higher than the vapour pressure of water (3.2 kPa at 25 °C). From this point of view, acetone might not be a suitable

201 solvent. Our results show that the required amine regeneration temperatures can be significantly reduced by using

202 non-aqueous solutions with small dielectric constants. However, it is important to look for a solvent with small

203 dielectric constant as well as low vapour pressure. One interesting solvent could be diethylene glycol monoethyl

204 ether (DEGMEE), which has dielectric constant of 15.6, which is very close to t-butanol included in our study.

205 DEGMEE has vapour pressure of 0.02 kPa which makes it a very good candidate. This explains why DEGMEE

206 was ranked as the best solvent in the recent experimental study conducted by Bougie et al.[8]

207 **III. CONCLUSION**

208 In this computational study we investigated the possibility of using non-aqueous solutions to reduce energy penalty

209 of amine regeneration in amine-based post-combustion carbon capture (PCCC) technology. We demonstrated the

210 ability of our computational framework to reproduce very well experimental activation energy of zwitterion

211 formation. We have shown that non-aqueous solutions with small dielectric constants are beneficial for more energy

212 efficient amine regeneration. From thermodynamics point of view, the change in regeneration enthalpy decreased

213 in the case of these non-aqueous solutions, suggesting less energy consumption in this case. Also in this case, the

214 reduction in activation energies will allow for running the desorption column at much lower temperatures. This

215 could enable us to completely rely on waste thermal energy instead of using expensive high-grade electrical heat

216 energy. Although these results are very promising, other factors such as the solvent volatility should be also

217 considered.

SUPPLEMENTARY MATERIAL

218 The Supplementary Material is available and contain activation energies (Table S1) and Gibbs free energies (Table

219 S2) of the different forward and backward reactions. These tables compare the values obtained purely from DFT

220 calculations to these obtained by combining coupled-cluster electronic energies and DFT vibrational frequency

221 calculations. Table S3 reports the evaluation of including the dispersion and geometrical counterpoise corrections.

ACKNOWLEDGMENTS

CONFLICTS OF INTEREST

The authors declare that there are no any conflicts of interest regarding the publication of this paper.

DATA AVAILABILITY

The data used to support the findings of this study are included within the article. Should further data or information be required, these are available from the corresponding author upon request.

REFERENCES

[1] Z. (Henry) Liang, W. Rongwong, H. Liu, K. Fu, H. Gao, F. Cao, R. Zhang, T. Sema, A. Henni, K. Sumon, D. Nath, D. Gelowitz, W. Srisang, C. Saiwan, A. Benamor, M. Al-Marri, H. Shi, T. Supap, C. Chan, Q. Zhou, M. Abu-Zahra, M. Wilson, W. Olson, R. Idem and P. (PT) Tontiwachwuthikul, Int. J. Greenh. Gas Control, 2015, 40, 26–54.

[2] S. J. McGurk, C. F. Martín, S. Brandani, M. B. Sweatman and X. Fan, Appl. Energy, 2017, 192, 126–133.

[3] G. T. Rochelle, Science (80-.)., 2009, 325, 1652–1654.

[4] K. Z. House, C. F. Harvey, M. J. Aziz and D. P. Schrag, Energy Environ. Sci., 2009, 2, 193.

[5] J. Husebye, A. L. Brunsvold, S. Roussanaly and X. Zhang, Energy Procedia, 2012, 23, 381–390.

[6] B. Dutcher, M. Fan and A. G. Russell, ACS Appl. Mater. Interfaces, 2015, 7, 2137–2148.

[7] C.-H. Yu, C.-H. Huang and C.-S. Tan, Aerosol Air Qual. Res., 2012, 12, 745–769.

[8] F. Bougie, D. Pokras and X. Fan, Int. J. Greenh. Gas Control, 2019, 86, 34–42.

[9] N. D. Afify and M. B. Sweatman, J. Chem. Phys., 2018, 148, 204513.

[10] N. D. Afify and M. B. Sweatman, J. Chem. Phys., 2018, 148, 024508.

[11] F. Bougie and X. Fan, Int. J. Greenh. Gas Control, 2018, 79, 165–172.

[12] N. D. Afify and M. B. Sweatman, J. Chem. Phys., 2019, 151, 024503.

[13] G. Rochelle, E. Chen, S. Freeman, D. Van Wagener, Q. Xu and A. Voice, Chem. Eng. J., 2011, 171, 725–733.

[14] S. Martin, H. Lepaumier, D. Picq, J. Kittel, T. de Bruin, A. Faraj and P.-L. Carrette, Ind. Eng. Chem. Res., 2012, 51, 6283–6289.

[15] A. Hartono, A. F. Ciftja, P. Brúder and H. F. Svendsen, Energy Procedia, 2014, 63, 2138–2143.

[16] E. Gjernes, L. I. Helgesen and Y. Maree, Energy Procedia, 2013, 37, 735–742.

[17] F. Closmann, T. Nguyen and G. T. Rochelle, Energy Procedia, 2009, 1, 1351–1357.

[18] F. Bougie and M. C. Iliuta, Ind. Eng. Chem. Res., 2010, 49, 1150–1159.

[19] B. Zhao, Y. Sun, Y. Yuan, J. Gao, S. Wang, Y. Zhuo and C. Chen, Energy Procedia, 2011, 4, 93–100.

[20] S.-W. Park, J.-W. Lee, B.-S. Choi and J.-W. Lee, Korean J. Chem. Eng., 2006, 23, 806–811.

[21] N. El Hadri, D. V. Quang, E. L. V. Goetheer and M. R. M. Abu Zahra, Appl. Energy, 2017, 185, 1433–1449.

[22] M. Lail, J. Tanthana and L. Coleman, Energy Procedia, 2014, 63, 580–594.

[23] M. Tao, J. Gao, P. Zhang, W. Zhang, Q. Liu, Y. He and Y. Shi, Energy & Fuels, 2017, 31, 6298–6304.

[24] F. J. Tamajón, E. Álvarez, F. Cerdeira and D. Gómez-Díaz, Chem. Eng. J., 2016, 283, 1069–1080.

[25] P. M. Mathias, F. Zheng, D. J. Heldebrant, A. Zwoster, G. Whyatt, C. M. Freeman, M. D. Bearden and P. Koech, ChemSusChem, 2015, 8, 3617–3625.

[26] M. Hasib-ur-Rahman and F. Larachi, Environ. Sci. Technol., 2012, 46, 11443–11450.

[27] R. Hart, P. Pollet, D. J. Hahne, E. John, V. Llopis-Mestre, V. Blasucci, H. Huttenhower, W. Leitner, C. A. Eckert and C. L. Liotta, Tetrahedron, 2010, 66, 1082–1090.

[28] M. Cui, S. Chen, T. Qi and Y. Zhang, J. Chem. Eng. Data, 2018, 63, 1198–1205.

[29] F. Barzagli, S. Lai and F. Mani, Energy Procedia, 2014, 63, 1795–1804.

[30] F. Barzagli, F. Mani and M. Peruzzini, Int. J. Greenh. Gas Control, 2013, 16, 217–223.

[31] V. Barone and M. Cossi, J. Phys. Chem. A, 1998, 102, 1995–2001.

[32] V. Barone and M. Cossi, J. Phys. Chem. A, 1998, 102, 1995–2001.

[33] M. J. Frisch, G. W. Trucks, H. B. Schlegel, G. E. Scuseria, M. A. Robb, J. R. Cheeseman, G. Scalmani, et al., Gaussian 16, Rev. C. 01, 2016.

[34] G. M. J. Barca, C. Bertoni, L. Carrington, D. Datta, N. De Silva, J. E. Deustua, D. G. Fedorov, J. R. Gour, et al., J. Chem. Phys., 2020, 152, 154102.

[35] F. Neese, F. Wennmohs, U. Becker and C. Riplinger, J. Chem. Phys., 2020, 152, 224108.

[36] T. Davran-Candan, J. Phys. Chem. A, 2014, 118, 4582–4590.

[37] S. Gangarapu, A. T. M. Marcelis, Y. A. Alhamed and H. Zuilhof, ChemPhysChem, 2015, 16, 3000–3006.

[38] E. Orestes, C. Machado Ronconi and J. W. de M. Carneiro, Phys. Chem. Chem. Phys., 2014, 16, 17213–17219.

[39] H.-B. Xie, Y. Zhou, Y. Zhang and J. K. Johnson, J. Phys. Chem. A, 2010, 114, 11844–11852.

[40] K. Z. Sumon, C. H. Bains, D. J. Markewich, A. Henni and A. L. L. East, J. Phys. Chem. B, 2015, 119, 12256–12264.

[41]H. M. Stowe and G. S. Hwang, Ind. Eng. Chem. Res., 2017, 56, 6887–6899.

[42]T. Zhang, Y. Yu and Z. Zhang, Mol. Simul., 2018, 44, 815–825.

[43]S. Kim, H. Shi and J. Y. Lee, Int. J. Greenh. Gas Control, 2016, 45, 181–188.

[44]B. Han, C. Zhou, J. Wu, D. J. Tempel and H. Cheng, J. Phys. Chem. Lett., 2011, 2, 522–526.

[45]Y. Matsuzaki, H. Yamada, F. A. Chowdhury, T. Higashii, S. Kazama and M. Onoda, Energy Procedia, 2013, 37, 400–406.

[46]Y. Matsuzaki, H. Yamada, F. A. Chowdhury, T. Higashii and M. Onoda, J. Phys. Chem. A, 2013, 117, 9274–9281.

[47]S. H. Ali, Int. J. Chem. Kinet., 2005, 37, 391–405.

[48]E. Alper, Ind. Eng. Chem. Res., 1990, 29, 1725–1728.

[49]S. Xu, Y.-W. Wang, F. D. Otto and A. E. Mather, Chem. Eng. Sci., 1996, 51, 841–850.

[50]G. Bruhn, E.R. Davidson, I. Mayer and A.E. Clark, Int. J. Quantum Chem., 2006, 106, 2065–2072.

[51]M.G. Evans, M. Polanyi, Trans. Faraday Soc., 1935, 31, 875–894.; H. Eyring, J. Chem. Phys., 1935, 3, 107–115.

[52]I. Sandler, J. Chen, M. Taylor, S. Sharma, and J. Ho, "Accuracy of DLPNO-CCSD(T): Effect of Basis Set and System Size," J. Phys. Chem. A 125(7), 1553–1563 (2021).

[53]L. Goerigk, A. Hansen, C. Bauer, S. Ehrlich, A. Najibi, and S. Grimme, "A look at the density functional theory zoo with the advanced GMTKN55 database for general main group thermochemistry, kinetics and noncovalent interactions," Phys. Chem. Chem. Phys. 19(48), 32184–32215 (2017).

[54]H. Kruse, and S. Grimme, "A geometrical correction for the inter- and intra-molecular basis set superposition error in Hartree-Fock and density functional theory calculations for large systems," J. Chem. Phys. 136(15), 154101- 154101 (2012).

[55]S. Grimme, S. Ehrlich, and L. Goerigk, "Effect of the damping function in dispersion corrected density functional theory," J. Comput. Chem. 32(7), 1456–1465 (2011).

[56]S. Grimme, S. Ehrlich, and L. Goerigk, "Effect of the damping function in dispersion corrected density functional theory," J. Comput. Chem. 32(7), 1456–1465 (2011).